Ultrabroadband terahertz radiation from low-temperature-grown GaAs photoconductive emitters

Y. C. Shen, P. C. Upadhya, E. H. Linfield,[a] and H. E. Beere
Cavendish Laboratory, University of Cambridge, Madingley Road, Cambridge, CB3 0HE United Kingdom

A. G. Davies
School of Electronic and Electrical Engineering, University of Leeds, Leeds, LS2 9JT United Kingdom

(Received 7 July 2003; accepted 21 August 2003)

Terahertz radiation was generated with a biased and asymmetrically excited low-temperature-grown GaAs photoconductive emitter, and characterized with a 20-μm-thick ZnTe crystal using free-space electro-optic sampling. Using a backward collection scheme, we obtained terahertz radiation with frequency components over 30 THz, the highest ever observed for photoconductive emitters. We present spectra over the whole frequency range between 0.3 and 20 THz, demonstrating the use of this source for ultrabroadband THz spectroscopy. © *2003 American Institute of Physics.*
[DOI: 10.1063/1.1619223]

The terahertz (THz) region of the electromagnetic spectrum spans the frequency range between the midinfrared and the millimeter/microwave (0.3–30 THz). Since the first use of femtosecond lasers to generate coherent THz radiation,[1] there has been a drive to develop higher power sources and systems of broader bandwidth.[2–4] A number of techniques including bulk electro-optic rectification,[5,6] surface field generation,[7,8] and ultrafast switching of photoconductive emitters,[9–13] have been explored. Of these different methods, photoconductive emitters have proved to be the most efficient technique for converting visible/near-IR pulses to THz radiation,[12,13] and have been widely used for THz spectroscopy and imaging. In this technique, electron-hole pairs are generated in the semiconductor crystal using an above-band gap femtosecond pulse, and these photoexcited carriers are then accelerated by an applied electric field. The physical separation of the electrons and holes forms a macroscopic space-charge field oriented opposite to the biasing field, and thus, the externally applied field is screened. The fast temporal change in electric field produces a transient current, which generates a pulse of electromagnetic radiation in the THz frequency range. Theoretical simulations using this electric field screening model suggest that sub-100 fs electrical pulses can be obtained.[14] In experiment, however, 200 fs electric pulses and 350 fs free-space THz pulses are amongst the shortest pulses realized for GaAs emitters, giving a useful bandwidth of about 4 THz.[4,9–13] Here we report that THz radiation with frequency components over 30 THz can be obtained from a biased and asymmetrically excited GaAs photoconductive emitter.

Figure 1 shows schematically the experimental arrangement for coherent generation and detection of THz radiation. The emitter comprised two vacuum-evaporated NiCr/Au electrodes separated by a 0.4 mm gap (Fig. 1, top right), deposited on a 1-μm-thick low-temperature-grown GaAs (LT-GaAs) layer on a 0.53-mm-thick undoped GaAs substrate. LT–GaAs was chosen to give a short photocarrier recombination lifetime (0.4 ps in this case), together with both high resistivity and high carrier mobility.[15] A bias voltage of ± 120 V, modulated at 31 kHz, was applied across the emitter. A pulsed Ti:sapphire laser of 300 mW average power (12 fs pulse width, 800 nm center wavelength, and 76 MHz repetition rate) was focused to a 40 μm spot diameter on the edge of one of the two NiCr/Au electrodes of the LT–GaAs emitter, to generate THz pulses. In contrast to previous experiments, where the THz radiation was collected forwards (that is after being transmitted through the GaAs substrate), we collected the THz radiation backwards (in the direction of the reflected pump laser beam, see Fig. 1, top left). As a

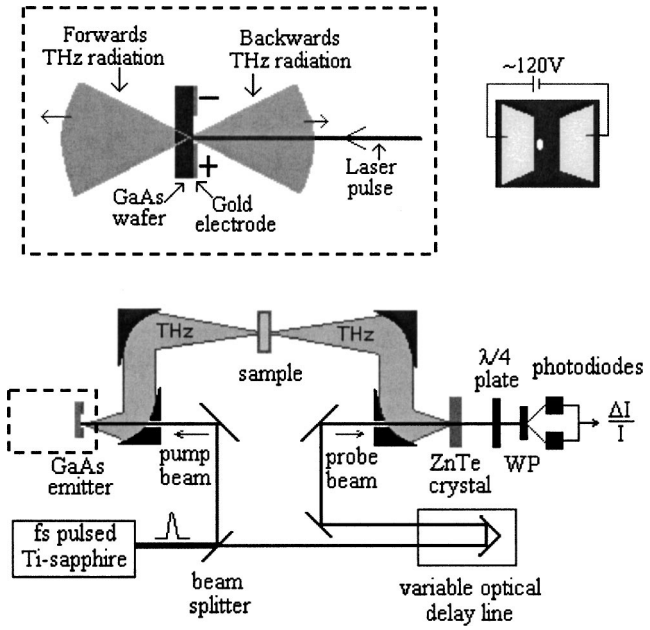

FIG. 1. Bottom: Experimental arrangement for coherent THz generation and detection. Top left: Generated THz radiation is emitted from both sides of the GaAs wafer. The backwards THz radiation is collected in our measurements, leading to the significantly enhanced bandwidth. Top right: Schematic geometry of the electrodes used in the biased GaAs photoconductive emitter. The white spot indicates the position of the asymmetric laser excitation.

[a]Electronic mail: ehl10@cam.ac.uk

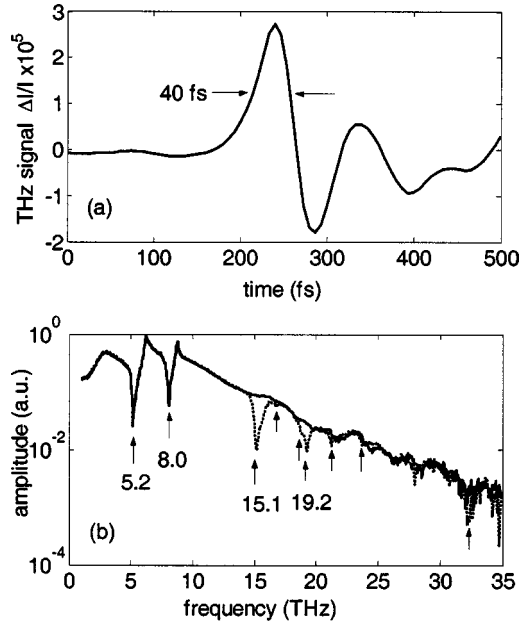

FIG. 2. (a) The temporal THz wave form and, (b) its corresponding Fourier-transform amplitude spectrum (upper trace, solid line), together with spectrum measured in the presence of PTFE sample (lower trace, dotted line).

result, the absorption and dispersion of the THz pulses in the GaAs substrate were minimized.

The emitted THz pulses were collimated and focused onto the sample by a pair of parabolic mirrors. The transmitted THz pulse (or in an alternative arrangement, this could be the reflected pulse) was then collected and focused using another pair of parabolic mirrors onto a 20-μm-thick (110) ZnTe crystal glued onto a 1-mm-thick wedged (100) ZnTe crystal for electro-optic detection.[16,17] In all measurements, the variable delay stage, which provides the time delay between the THz pulse and the probe pulse, was scanned over a distance of 2 mm, providing a spectral resolution of 75 GHz ($2.5\,\mathrm{cm}^{-1}$). Using a lock-in detection scheme referenced to the frequency of the bias across the GaAs emitter, we observed a noise level equivalent to $\Delta I/I = 8 \times 10^{-9}\ \mathrm{Hz}^{-1/2}$. With this noise level, peak signals obtained in our experiments are as much as a factor of 1400 above the noise floor. The apparatus shown in Fig. 1 was enclosed in a vacuum-tight box, which was purged with dry nitrogen gas to reduce the effects of water vapor absorption. All measurements were performed at room temperature.

Figure 2(a) shows a typical resulting temporal THz waveform, with Fig. 2(b) showing the corresponding frequency spectrum. The first main positive and negative peaks of the pulse [Fig. 2(a)] have full width at half maxima of 40 and 35 fs, respectively, representing the shortest THz pulses reported for photoconductive emitters.[9–13] The spectral dips at 5.2 and 8.0 THz [Fig. 2(b)] are caused by absorptions in the ZnTe detector (TO phonon energy: 22 meV$\equiv$5.3 THz) and the GaAs emitter (TO phonon energy: 33 meV $\equiv$8.0 THz),[18] respectively. Note that frequency components over 30 THz are observed. These represent the highest frequency components reported from a biased photoconductive emitter, and are a direct consequence of the use of the reflection geometry.

Figure 2(b) also shows (lower trace) the amplitude spectrum of the THz signal measured after transmission through a polytetrafluroethylene (PTFE) sample (Thermo Co., UK). A number of spectral features are observed, in particular two strong dips at 15.1 and 19.2 THz, caused by absorption owing to CF_2 scissoring and wagging vibrations, respectively. In addition, a weak absorption feature at 16.7 THz (CF_2 twisting vibration) and a shoulder at 18.8 THz (CF_2 wagging vibration) are also visible. Above 20 THz, the measured spectrum became noisy. However, absorption features around 21.2, 23.7, and 32.3 THz are still visible, corresponding to two symmetric stretching vibrations of CF_2, and the symmetric stretching vibration of SO_3^-, respectively. These values agree well with the published data,[19] demonstrating the useful bandwidth of our THz spectrometer.

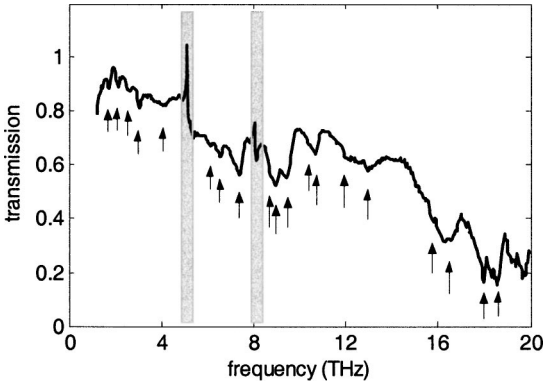

FIG. 3. Transmission spectrum of the cytidine sample. Two shaded areas centred at 5.1 and 8.0 THz contain singularities caused by the TO phonons of the ZnTe and GaAs crystals, respectively. Arrows indicate vibrational modes at frequencies of 1.7, 2.1, 2.5, 3.0, 4.1, 6.1, 6.5, 7.4, 8.7, 8.9, 9.4, 10.7, 12.1, 13.0, 15.6, 16.6, 17.9, and 18.6 THz.

An alternative approach for broadband THz generation is optical rectification of femtosecond Ti:sapphire laser pulses at the surface of a nonlinear optic crystal or semiconductor. The spectrum of such a source is also broad extending in principle from zero frequency to over 30 THz.[5] However, owing to lack of phase matching it exhibits only low average power. Higher average power can be obtained by phase-matched difference frequency mixing in nonlinear crystals such as GaSe. The THz radiation generated is tunable from far-IR to mid-IR by changing the crystal orientation to achieve phase matching for a given frequency component.[6,20]

We also note that, in comparison with published results on GaAs *p-i-n* vertical diodes,[17] where frequency components as high as 60 THz have been observed, our LT–GaAs emitter provides two to three orders of magnitude higher THz power (estimated from the published $\Delta I/I$ value).[17,21] (It should be noted, however, that higher THz power does not necessary mean higher conversion efficiency because the GaAs *p-i-n* diodes used less pump laser power.) Furthermore, our LT–GaAs emitter can be operated at much higher chopping frequencies, essential for practical applications such as ultrabroadband THz spectroscopy and spectrally resolved THz imaging.

To demonstrate further the capability of our broadband THz spectroscopy system in probing both intra- and intermolecular vibrations, the THz transmission spectrum of polycrystalline cytidine was measured and is shown in Fig. 3. Cytidine is one of four nucleosides found in RNA and DNA,

and polycrystalline samples contain an extensive network of intermolecular hydrogen bonds.[22,23] Polycrystalline cytidine (EC No. 2006109) was purchased from Sigma-Aldrich and had a purity of 99%. Samples for THz measurements were prepared by forming a thin layer of finely milled cytidine powder between two transparent 9-μm-thick polyethylene films. Nineteen vibrational modes were observed in the frequency range 1–20 THz. Amongst these, five (12.1, 13.0, 16.6, 17.9, 18.6 THz) have been observed previously using Fourier-transform infrared spectroscopy.[24] Our THz measurements, however, provide a broader spectral coverage (1–20 THz), and reveal more vibrational modes. These include so-called external or lattice modes involving the motion of molecules moving relative to each other in the unit cell of the cytidine crystal. The accurate calculation and assignment of such vibrational modes is difficult and requires the inclusion of noncovalent long-range weak forces including hydrogen bonds.[22,25] Indeed, although these forces play a pivotal rule in biomolecular structure and function, they are poorly understood at this time. The rich spectral features of the THz spectrum reported here provide important information to help understand better the nature of such forces.

Raman spectroscopy has also resolved fourteen vibrational modes of cytidine below 20 THz.[26] However, the THz and Raman spectral data are in general complementary. Depending on the nature of the vibration, which is determined by the symmetry of the molecule, vibrations may be active or forbidden in the IR or Raman spectra. Neutron inelastic scattering (NIS) spectroscopy, on the other hand, is in principle sensitive to all vibrational motions, and therefore should be able to reveal all vibrational modes of cytidine. However, only twelve vibrational modes below 20 THz were resolved in NIS measurements.[22,26] This is partly a result of the limited spectral resolution ($\sim 1\ \mathrm{THz} \equiv 33\ \mathrm{cm}^{-1}$) achieved in the measurements. In addition, NIS spectroscopy is most sensitive to vibrational modes involving hydrogen displacements, owing to the high cross section of the hydrogen atoms in the NIS process. As a result, vibrational modes arising from heavy atom (C, N, O, and P) vibrations, which can be probed by optical spectroscopy (Raman scattering and IR absorption), may not be resolved in NIS measurements.

In conclusion, we have reported the generation of broadband THz radiation from a LT–GaAs photoconductive emitter, and demonstrated the use of this powerful source for broadband (over 20 THz) THz spectroscopy. This extended frequency range is immediately useful for time-resolved THz spectroscopy, and provides important information on the vibrational modes arising from both intra- and intermolecular interactions. We also note that the time-resolved nature of this system provides a unique tool for pump-probe studies of the dynamical properties of materials in the mid-IR and far-IR frequency ranges.[27,28]

The authors thank I. Gregory and C. Baker for characterizing the LT–GaAs wafers. This work was supported by the EPSRC (UK), the Royal Society, and Toshiba Research Europe Ltd.

[1] D. H. Auston, K. P. Cheung, and P. R. Smith, Appl. Phys. Lett. **45**, 284 (1984).
[2] See, for example, M. C. Nuss and J. Orenstein, in *Millimeter and Submillimeter Wave Spectroscopy of Solids*, edited by G. Grüner, (Berlin, Springer, 1998), and references therein.
[3] B. Ferguson and X.-C. Zhang, Nat. Mater. **1**, 26 (2002).
[4] M. C. Beard, G. M. Turner, and C. A. Schmuttenmaer, J. Phys. Chem. B **106**, 7146 (2002).
[5] Q. Wu and X.-C. Zhang, Appl. Phys. Lett. **71**, 1285 (1997).
[6] R. A. Kaindl, F. Eickemeyer, M. Woerner, and T. Elsaesser, Appl. Phys. Lett. **75**, 1060 (1999).
[7] T. Dekorsy, H. Auer, H. J. Bakker, H. G. Roskos, and H. Kurz, Phys. Rev. B **53**, 4005 (1996).
[8] A. G. Davies, E. H. Linfield, and M. B. Johnston, Phys. Med. Biol. **47**, 3679 (2002).
[9] D. Krokel, D. Grischkowsky, and M. B. Ketchen, Appl. Phys. Lett. **54**, 1046 (1989).
[10] U. D. Keil and D. R. Dykaar, Appl. Phys. Lett. **61**, 1504 (1992).
[11] N. Katzenellenbogen and D. Grischkowsky, Appl. Phys. Lett. **58**, 222 (1991).
[12] I. Brener, D. Dykaar, A. Frommer, L. N. Pfeiffer, J. Lopata, J. Wynn, K. West, and M. C. Nuss, Opt. Lett. **21**, 1924 (1996).
[13] G. Zhao, R. N. Schouten, N. van der Valk, W. Th. Wenckebach, and P. C. M. Planken, Rev. Sci. Instrum. **73**, 1715 (2002); Phys. Med. Biol. **47**, 3699 (2002).
[14] E. Sano and T. Shibata, Appl. Phys. Lett. **55**, 2748 (1989).
[15] K. Zhang and D. L. Miller, J. Electron. Mater. **22**, 1433 (1993).
[16] Q. Wu and X.-C. Zhang, Appl. Phys. Lett. **70**, 1784 (1997).
[17] A. Leitenstorfer, S. Hunsche, J. Shah, M. C. Nuss, and W. H. Knox, Appl. Phys. Lett. **74**, 1516 (1999).
[18] M. Tani, R. Fukasawa, H. Abe, K. Sakai, and S. Nakashima, J. Appl. Phys. **83**, 2473 (1998).
[19] A. Gruger, A. Regis, T. Schmatko, and P. Colomban, Vib. Spectrosc. **26**, 215 (2001).
[20] R. Huber, A. Brodschelm, F. Tauser, and A. Leitenstorfer, Appl. Phys. Lett. **76**, 3191 (2000).
[21] A. Leitenstorfer, S. Hunsche, J. Shah, M. C. Nuss, and W. H. Knox, Phys. Rev. Lett. **82**, 5140 (1999); Phys. Rev. B **61**, 16642 (2000).
[22] M. Plazanet, N. Fukushima, and M. R. Johnson, Chem. Phys. **280**, 53 (2002).
[23] B. Fischer, M. Malther, and P. Uhd Jepsen, Phys. Med. Biol. **47**, 3807 (2002).
[24] M. Rozenberg, C. Jung, and G. Shoham, Phys. Chem. Chem. Phys. **5**, 1533 (2003).
[25] N. Leulliot, M. Ghomi, H. Jobic, O. Bouloussa, V. Baumruk, and C. Coulombeau, J. Phys. Chem. B **103**, 10934 (1999).
[26] M. Mathlouthi, A. M. Seuvre, and J. L. Koenig, Carbohydr. Res. **146**, 1 (1986).
[27] R. Huber, F. Tauser, A. Brodschelm, M. Bichler, G. Abstreiter, and A. Leitenstorfer, Nature (London) **414**, 286 (2001).
[28] A. H. Xie, A. F. G. van der Meer, and R. H. Austin, Phys. Rev. Lett. **88**, 018102 (2002).